PHYSICAL REVIEW D **85,** 123001 (2012)

Cosmological constraints on nonstandard inflationary quantum collapse models

Susana J. Landau*
Instituto de Física de Buenos Aires, CONICET-UBA, Ciudad Universitaria-Pab. 1, 1428 Buenos Aires, Argentina

Claudia G. Scóccola
Instituto de Astrofísica de Canarias (IAC), C/Vía Láctea, s/n, E-38200, La Laguna, Tenerife, Spain. Dpto. Astrofísica, Universidad de La Laguna (ULL), E-38206 La Laguna, Tenerife, Spain

Daniel Sudarsky
Instituto de Ciencias Nucleares, Universidad Nacional Autónoma de México, A. Postal 70-543, México D. F. 04510, México
(Received 7 December 2011; published 4 June 2012)

We briefly review an important shortcoming—unearthed in previous works—of the standard version of the inflationary model for the emergence of the seeds of cosmic structure. We consider here some consequences emerging from a proposal inspired on ideas of Penrose and Diósi [R. Penrose, *The Emperor's New Mind. Concerning Computers, Minds and Laws of Physics* (1989).][R. Penrose, in *Physics meets Philosophy at the Planck Scale: Contemporary Theories in Quantum Gravity*, edited by C. Callendar and N. Huggett (2001), pp. 290–+.][L. Diósi, Phys. Lett. A **120**, 377 (1987).][L. Diósi, Phys. Rev. A **40**, 1165 (1989).] about a quantum-gravity induced reduction of the wave function, which has been put forward to address the shortcomings, arguing that its effect on the inflaton field is what can lead to the emergence of the seeds of cosmic structure [A. Perez, H. Sahlmann, and D. Sudarsky, Classical Quantum Gravity **23**, 2317 (2006).]. The proposal leads to a deviation of the primordial spectrum from the scale-invariant Harrison-Zel'dovich one, and consequently, to a different CMB power spectrum. We perform statistical analyses to test two quantum collapse schemes with recent data from the CMB, including the 7-yr release of WMAP and the matter power spectrum measured using LRGs by the Sloan Digital Sky Survey. Results from the statistical analyses indicate that several collapse models are compatible with CMB and LRG data, and establish constraints on the free parameters of the models. The data put no restriction on the timescale for the collapse of the scalar field modes.

DOI: 10.1103/PhysRevD.85.123001 PACS numbers: 98.70.Vc, 98.80.Cq

I. INTRODUCTION

The great advances made in physical cosmology over the past few years open a window for the consideration of issues long dismissed as philosophical speculations. The agreement between theory and observations of the spectrum of the cosmic microwave background (CMB) anisotropies has strengthened the theoretical status of inflationary scenarios among cosmologists. The inflationary paradigm is said to account for the origin of all cosmic structure: the fluctuations around homogeneity and isotropy that have a fundamentally quantum nature are, according to these ideas, the seeds of galaxies, stars, life and humans. Hence, all structures in our universe emerge from a featureless stage described by a background Friedmann-Robertson-Walker (FRW) cosmology with a nearly exponential expansion driven by the potential of a single scalar field,[1] and from its quantum fluctuations characterized by a simple vacuum state. In particular, the quantum fluctuations transmute into the classical statistical fluctuations that imprint their signature in the CMB photons, and eventually grow into the structures we find in our universe today.

However, when this picture is considered thoroughly, an unavoidable issue arises. According to these ideas, a completely homogeneous and isotropic stage, somehow evolves, after some time, into an inhomogeneous and anisotropic situation. Obviously, this is not simply the result of quantum unitary evolution, since, in this case, the dynamics does not break the initial symmetries of the system. As discussed in Ref. [1], and despite multiple claims to the contrary, there is no satisfactory solution to this problem within the standard physical paradigms. While much of the focus of the research in inflationary cosmology has been directed towards elucidation of the details of the inflationary model, very little attention has been given by the community to an issue of fundamental principles such as the aforementioned one.

One proposal to handle this shortcoming has been developed in Refs. [2–4]. That approach attempts to deal with the problem by introducing a new ingredient into the inflationary account of the origin of the seeds of cosmic structure: *the self induced collapse hypothesis*, i.e. a scheme in which an internally induced collapse of the wave function of the inflaton field[2] is the mechanism by which inhomogeneities

*Member of the Carrera del Investigador Científica y Tecnológica - CONICET

[1]In the simplest models of inflation: ϕ, the inflaton.

[2]As shown in [5], one can implement the collapse hypothesis at the level of the Mukhanov Sasaki variable.

and anisotropies arise at each particular length scale. That work was inspired in early ideas by R. Penrose and L. Diósi [6–9] which regarded the collapse of the wave function as an actual physical process (instead of just an artifact of the description of Physics) and it is assumed to be caused by quantum aspects of gravitation. We will not recapitulate the motivations and discussion of the original proposal but instead refer the reader to the above mentioned papers.

The way we treat this process is by assuming that at a certain stage in cosmic evolution there is an induced jump in a state describing a particular mode of the quantum field, in a manner that is similar to the quantum mechanical reduction of the wave function associated with a measurement, but with the difference that in our scheme no external measuring device or observer is called upon as triggering such collapse (as there is nothing in the situation we are considering that could be called upon to play such a role). The issue that then arises concerns the characteristics of the state into which such jump occurs. In particular, what determines the expectation values of the field and momentum conjugate variables for the after-collapse state. Previous works by people in our group have extensively discussed both the conceptual and formal aspects of that problem, and the present manuscript will not dwell further into those aspects, except for a very short review.

In Ref. [2] two schemes were considered; one in which, after the collapse, both expectation values are randomly distributed within their respective ranges of uncertainties in the precollapsed state, and another one in which it is only the conjugate momentum that changes its expectation value from zero to a value in its corresponding range, as a result of the collapse. We will discuss the motivations and detailed characterizations of the two processes in the following sections. As reported in Ref. [2], the different collapse schemes give rise to different characteristic departures from the conventional Harrison-Zel'dovich (HZ) flat primordial spectrum.

These aspects have been preliminarily analyzed in Ref. [10] using a simple approach which ignores the late-time physics effects and simply considers what can be a reasonable expectation for the allowed deviation from the conventional flat spectrum. The main objective of this article is to consider in detail the shape of the primordial spectrum emerging from such a scheme, and, in particular, to explore with precision the deviations that should be expected once one takes into account the physics associated with plasma dynamics, which is responsible for the generation of the acoustic peaks, and other modifications to the spectrum associated with well established physics. All of these must be taken into account so that one can compare directly the predictions corresponding to a particular collapse model to recent data from the CMB fluctuation spectrum and the matter power spectrum from recent galaxy surveys, and thus be able to put bounds on the model's parameters.

The paper is organized as follows. In Sec. II, we describe the theoretical framework in which to study the models to be tested. Section III gives some specifications about the proposed collapse schemes together with a brief physical motivation for them, while Sec. IV is dedicated to general predictions of these models, and a broad comparison to observational data. We define a fiducial model which is determined by the best fit values obtained by the WMAP collaboration with the same data used in this paper and without assuming any collapse of the wave function. It should be noted that the fiducial model has a value of the spectral scalar index n_s different than 1, while calculations we have carried out here of the primordial fluctuation spectrum for models including collapse are restricted to the case $n_s = 1$. In Sec. V, we use data from WMAP 7-year release and the power spectrum of the Sloan Digital Sky Survery DR7 LRG, to put bounds on the free parameters of the collapse models, allowing also other cosmological parameters to vary. In Sec. VI, we discuss our results and show our conclusions.

II. THE FORMALISM/THEORETICAL MODEL

The starting point is the same as for the standard approaches, and, in particular, we will focus on one of the simplest inflationary models corresponding to a single scalar field, minimally coupled to gravity, with an appropriate potential. The action for the theory is

$$S[\phi, g_{ab}] = \int d^4x\sqrt{-g}\Big(\frac{1}{16\pi G}R[g_{ab}] - \frac{1}{2}\nabla_a\phi\nabla_b\phi g^{ab} - V(\phi)\Big). \quad (1)$$

As it is customary in such studies, we separate the fields into a "background" part, taken to be homogeneous and isotropic, FRW universe driven by an equally homogeneous and isotropic configuration of the inflaton field, and the perturbations (or "fluctuations").[3] In this way, the metric and the scalar field are written as: $g = g_0 + \delta g$ and $\phi = \phi_0 + \delta\phi$. This perturbative treatment requires, as usual, to deal with the gauge freedom, which we do by fixing the gauge (conformal Newton gauge). In the present work, we will ignore the vector and tensor parts of the metric perturbations. The space-time metric is described as: $ds^2 = a(\eta)^2[-(1+2\phi)d\eta^2 + (1-2\Psi)\delta_{ij}dx^i dx^j]$, where Ψ and ϕ are the *Newtonian potentials*. In this case, as it is well-known [2] the field equations imply $\phi = \Psi$. The scale factor a is normalized so that today $a = 1$.

[3]In fact, the proposal has been developed to fit within a semiclassical treatment where gravitation is treated at the classical level but the scalar fields are completely described using quantum field theory on curved space-time in a self-consistent approach adapted to incorporate the collapse hypothesis. For a detailed description of this approach see [11].

In order to further specify the setting of the problem, let us recall the standard inflationary version of cosmology. The universe is thought to go through the following epochs: 1) A quantum gravity regime which leads to 2) a preinflationary classical space-time which in turns enters 3) an inflationary regime with $a = a_{\rm BI}$ (BI stands for ''beginning of inflation'') and that ends when $a = a_{\rm EI}$ (EI stands for ''end of inflation''), passing through a rapid 4) reheating period, taken in our approximation to occur instantaneously. The next epoch is 5) a radiation-dominated era starting at $a = a_{\rm EI}$, with the radiation characterized by a temperature $T = T_{\rm GUT}$, and ending at the transition $a_{\rm eq}$ where 6) the matter (and later also the dark energy) era begins. Particularly interesting for us will be the recombination time occurring during the radiation-dominated regime, with $a = a_D$ and whose intersection with our past light-cone defines the surface of last scattering that is observed today in the CMB.

We will use a different conformal time coordinate for each of the eras. Thus, we will use η as the conformal time during inflation, $\tilde{\eta}$ the conformal time during radiation epoch and $\bar{\eta}$ the conformal time during the matter and dark energy epochs, and therefore the values of these coordinates at the transition points will generally differ.

We choose the origin of η so that during inflation we have $a = \frac{-1}{H_I \eta}$, thus inflation will end at $\eta = \eta_{\rm EI} = \frac{-1}{H_I a_{\rm EI}} < 0$. On the other hand, we choose the radiation-dominated era to start at $\tilde{\eta} = 0$ so that during the radiation epoch $a = C\tilde{\eta} + B$, with $C = [\frac{8\pi G}{3}(\rho_{\rm Rad} a^4)]^{1/2}$ and $B = a_{\rm EI}$, where $\rho_{\rm Rad}$ is the radiation energy density so that $\rho_{\rm Rad} a^4$ is constant during the era of radiation domination. Note that we are considering the reheating to occur instantaneously and hence the end of inflation (at $\eta = \eta_{\rm EI}$) and the start of radiation dominated era (at $\tilde{\eta} = 0$) coincide, so that $B = a_{\rm EI}$.

The study will rely on Einstein Field Equations (EFE) to zeroth and first order. The zeroth order gives rise to the standard solutions in the inflationary stage, where $a(\eta) = -\frac{1}{H_I \eta}$, with $H_I^2 \simeq (8\pi/3)$ GV with the scalar field ϕ_0 in slow-roll regime, so that $\phi_0' \simeq -\frac{1}{3H_I}\frac{dV}{d\phi}$; and the first order EFE leads to an equation relating the gravitational perturbation and the perturbation of the field:

$$\nabla^2 \Psi = 4\pi G \phi_0' \delta\phi' \equiv s\delta\phi', \tag{2}$$

where $s \equiv 4\pi G \phi_0'$. Next, we must consider the quantization of the inflaton perturbation field. It is convenient to work with the rescaled field $y = a\delta\phi$. In order to avoid infrared problems, we consider the system restricted to a box of side L, where we impose, as usual, periodic boundary conditions. We thus write the fields as

$$\begin{aligned} \hat{y}(\eta, \vec{x}) &= \frac{1}{L^3}\sum_k e^{i\vec{k}\cdot\vec{x}} \hat{y}_k(\eta), \\ \hat{\pi}(\eta, \vec{x}) &= \frac{1}{L^3}\sum_k e^{i\vec{k}\cdot\vec{x}} \hat{\pi}_k(\eta), \end{aligned} \tag{3}$$

where $\hat{\pi}_k$ is the canonical momentum of the scaled field. The wave vectors satisfy $k_i L = 2\pi n_i$, with $i = 1, 2, 3$. Also, as usual, we write the field operators in terms of the time-independent creation and annihilation operators, $\hat{y}_k(\eta) \equiv y_k(\eta)\hat{a}_k + \bar{y}_k(\eta)\hat{a}_k^\dagger$, and $\hat{\pi}_k(\eta) \equiv g_k(\eta)\hat{a}_k + \bar{g}_k(\eta)\hat{a}_k^\dagger$. The functions $y_k(\eta), g_k(\eta)$ reflect the selection of the vacuum state, and here we again proceed as in the standard approaches and choose the so called Bunch-Davies vacuum:

$$y_k(\eta) = \frac{1}{\sqrt{2k}}\left(1 - \frac{i}{\eta k}\right)e^{-ik\eta}, \qquad g_k(\eta) = -i\sqrt{\frac{k}{2}}e^{-ik\eta}. \tag{4}$$

The vacuum state, defined by $\hat{a}_k|0\rangle = 0$ for all k, is exactly homogeneous and isotropic. We assume that at a certain time η_k^c the part of the state characterizing the mode $\vec{k}$ (we must of course be aware that the state of the field is a collective state of all modes but taking here in this loose sense will do no harm) jumps to a new state, which is no longer homogeneous and isotropic. The detailed description of this process is as follows.

We decompose the fields into their hermitian part as: $\hat{y}_k = \hat{y}_k^R(\eta) + i\hat{y}_k^I(\eta)$, and $\hat{\pi}_k = \hat{\pi}_k^R(\eta) + i\hat{\pi}_k^I(\eta)$. We note that the vacuum state $|0\rangle$ is characterized in part by the following: its expectation values are $\langle\hat{y}_k^{R,I}(\eta)\rangle = \langle\hat{\pi}_k^{R,I}(\eta)\rangle = 0$, and its uncertainties are $\Delta\hat{y}_k^{R,I} = 1/2|y_k|^2(\hbar L^3)$ and $\Delta\hat{\pi}_k^{R,I} = 1/2|g_k|^2(\hbar L^3)$.

According to the collapse hypothesis, at some appropriate time $\eta_{\vec{k}}^c$, the state undergoes an instantaneous jump to a different state so that the mode $\vec{k}$ is not longer in its vacuum state.

For any state of the field $|\Omega\rangle$, we introduce the quantity $d_k \equiv \langle\Omega|\hat{a}_k^{R,I}|\Omega\rangle \equiv |d_k^{R,I}|e^{i\alpha_k}$ so that, for that state, we have

$$\langle\hat{y}_k^{R,I}\rangle = \sqrt{2}\Re(y_k d_k^{R,I}), \qquad \langle\hat{\pi}_k^{R,I}\rangle = \sqrt{2}\Re(g_k d_k^{R,I}), \tag{5}$$

indicating that it specifies the main quantity of interest in characterizing the state of the field.

The analysis proceeds with the specification of the scheme of collapse determining the state of the field after the collapse.[4] The detailed characterization of the schemes under consideration is the main purpose of the next section. With such a collapse scheme at hand, one then proceeds to evaluate the perturbed metric using a semiclassical description of gravitation in interaction with quantum fields as reflected in the semiclassical EFEs: $G_{ab} = 8\pi G\langle T_{ab}\rangle$ (see Eq. (2) for the classical first order version). To lowest order, and for the quantity of interest, this set of equations reduces to

[4]At this point, in fact, all we require is the specification of the expectation values of certain operators in this new quantum state.

$$\nabla^2\Psi_k = s\langle\delta\hat{\phi}'_k\rangle_\Omega, \tag{6}$$

where $\langle\delta\hat{\phi}'_k\rangle_\Omega$ is the expectation value of the momentum field $\delta\hat{\phi}'_k = \hat{\pi}_k/a(\eta)$ on the state $|\Omega\rangle$ characterizing the quantum part of the inflaton field. It is worthwhile emphasizing that *before* the collapse has occurred *there are no* metric perturbations, i.e. the r.h.s. of the last equation evaluated on the vacuum state is zero, so, it is only *after* the collapse that the gravitational perturbations appear, i.e. the collapse of each mode represents the onset of the inhomogeneity and anisotropy at the scale represented by the mode. Another point we must stress is that, according to our views, at all times, the *Universe would be defined by a single state and not by an ensemble of states. The precise state at any time, could be written if we knew the modes that have collapsed up to that time, and the post-collapse states for each of these modes.* The statistical aspects arise once we note that we do not measure directly and separately each of the modes with specific values of $\vec{k}$, but rather the aggregate contribution of all such modes to the spherical harmonic decomposition of the temperature fluctuations of the celestial sphere (see below).

In order to be able to compare to observations we note that the quantity that is experimentally measured (for instance by WMAP satellite) is the anisotropy in the temperature, $\Delta T(\theta, \varphi)/T$, which is expressed in terms of its spherical harmonic decomposition as $\sum_{lm} a_{lm} Y_{lm}(\theta, \varphi)$. The link to theoretical calculations is made through the theoretical estimation of the value of the a_{lm}'s, which are expressed in terms of the Newtonian potential on the 2-sphere corresponding to the intersection of our past light cone with the last scattering surface (LSS): $\Psi(\eta_D, \vec{x}_D)$, $a_{lm} = \int \Psi(\eta_D, \vec{x}_D) Y^*_{lm} d^2\Omega$. We must then consider the expression for the Newtonian potential (Eq. (6)) at those points:

$$\Psi(\eta, \vec{x}) = \sum_k \frac{s\mathcal{T}(k)}{k^2 L^3}\langle\delta\hat{\phi}'_k\rangle e^{i\vec{k}\cdot\vec{x}}, \tag{7}$$

where we have introduced the factor $\mathcal{T}(k)$ to represent the physical effects of the period between reheating and decoupling.

Writing the coordinates of the points of interest on the surface of last scattering as $\vec{x} = R_D(\sin\theta\sin\phi, \sin\theta\cos\phi, \cos\theta)$, where R_D is the comoving radius to that surface, and (θ, ϕ) are the standard spherical coordinates on the sphere, and using standard results connecting Fourier and spherical expansions, we obtain

$$a_{lm} = \sum_k \frac{s\mathcal{T}(k)}{k^2 L^3}\int\langle\delta\hat{\phi}'_k\rangle e^{i\vec{k}\cdot\vec{x}} Y_{lm}(\theta, \phi) d^2\Omega. \tag{8}$$

As indicated above, statistical considerations arise when noting that Eq. (8) indicates that the quantity of interest is in fact the result of a large number (actually infinite) of harmonic oscillators, each one contributing with a complex number to the sum, leading to what is in effect a two dimensional random walk whose total displacement corresponds to the quantity of observational interest. Note that this part of the analysis is substantially different from the corresponding one in the standard approach. In order to obtain a prediction, we need to find the *magnitude* of such total displacement, i.e. $|a_{lm}|^2$, and given that by assumption there are multiple random processes involved, the best that can be obtained is the "most likely" value for this quantity (just as in a random walk one can not expect to predict the actual value but at best its most likely value). We do this with the help of the *imaginary* ensemble of universes[5] and the identification of the most likely value with the ensemble mean value. We should emphasize however that if we knew the specific values taken by the random numbers x we will specify below, we would be able to compute explicitly the value of each a_{lm} including the phase.

As we will see, the ensemble mean value of the product $\langle\delta\hat{\phi}_k\rangle\langle\delta\hat{\phi}_{k'}\rangle^*$, evaluated in the post-collapse states,[6] results in a form $\kappa C(k)\delta_{\vec{k}\vec{k}'}$, where $\kappa = \hbar L^3 k/(4a^2)$ and $C(k)$ is an adimensional function of k which encodes the relevant information of detailed aspects of the collapse scheme. Then, using the expression for $|a_{lm}|^2$, writing the sum as an integral, and doing a change of integration variable $x = kR_D$, we arrive to the following expression for the most likely (ML) value of the quantity of interest:

$$|a_{lm}|^2_{\mathrm{ML}} = \frac{s^2\hbar}{2\pi a^2}\int\frac{C(x/R_D)}{x}\mathcal{T}(x/R_D)^2 j_l^2(x)dx. \tag{9}$$

With this expression at hand, we can compare the expectations from each of the schemes of collapse against the observations. We note, in considering the last equation, that the standard form of the spectrum corresponds to replacing the function C by a constant. In fact if one replaces C by 1 and, furthermore, one takes the function $\mathcal{T}$ which encodes the late-time physics including the plasma oscillations which are responsible for the famous acoustic peaks, and substitutes it by a constant, one obtains the characteristic signature of a scale invariant spectrum: $|a_{lm}|^2_{\mathrm{ML}} \propto \frac{1}{l(l+1)}$. Maintaining the appropriate function $\mathcal{T}$ leads of course to the well-known spectral shape that fits the data quite well once some basic cosmological parameters have been appropriately adjusted.

In the remainder of the paper, we will focus on the effects that a nontrivial form of the function C has on the predicted form of the observational spectrum, and on using data to constrain aspects of the collapse models.

[5]This is just a mathematical evaluation device and no assumption regarding the existence of such ensemble of universes is made or needed. These aspects of our discussion can be regarded as related to the so called cosmic variance problem.

[6]Note here again the difference with the standard treatment of this part of the calculation, which calls for the evaluation of the expectation value $\langle\delta\hat{\phi}_k\delta\hat{\phi}_{k'}\rangle^*$ on the vacuum state which as already emphasized is completely homogeneous and isotropic.

III. DESCRIPTION OF THE PROPOSED COLLAPSE SCHEMES

A collapse scheme is a recipe to characterize and select the state into which each of the modes $\vec{k}$ of the scalar field jumps at the corresponding time of collapse $\eta_{\vec{k}}^c$.

As we have clearly stated, we do not know exactly what kind of physical mechanism would lie behind what, at the semiclassical level we are working, looks like a spontaneous collapse of the wave function. Thus, specifying the collapse scheme should be taken as being at this point purely guesswork, which we hope to address with as much physical intuition as possible. The aspect that makes such efforts worthwhile is the fact that, as we shall see, the various specific collapse schemes lead generically to different generic patterns of deviations of the form of the primordial spectrum from the standard HZ scale-free shape.

The differences in the form of the primordial spectrum lead in turn to characteristic deformations for the predictions of the observational spectrum which is the result of late-time and well understood physical effects on the primordial spectrum. Thus, observations can help us to determine which one of the naively guessed collapse schemes is favored by the data.

In this paper, we focus on two schemes which we characterize simply in terms of the expectation values of the fundamental field operators (field and momentum conjugated) for the various modes in the state just after the corresponding collapse. It turns out that this limited characterization of the state (together with the times of the collapses) is all one needs to compute the shape of the expected spectrum. The higher level characterization of the states, such as the uncertainties and field-momentum correlations, turns out to be relevant only when one considers the possibility of multiple collapses per mode (see [12]) something that lies outside the scope of the present work.

Scheme I: It is the scheme where both the expectation value of the field and the expectation value of the conjugated momentum change as a result of the collapse in a random uncorrelated manner dictated by the uncertainties of the precollapse state, so that, immediately after the collapse time η_k^c, the expectation values are determined by

$$\begin{aligned}\langle \hat{y}_k^{(R,I)}(\eta_k^c)\rangle_\Omega &= x_1^{(R,I)}\sqrt{(\Delta y_k^{(R,I)})_0^2},\\ \langle \hat{\pi}_k^{(R,I)}(\eta_k^c)\rangle_\Omega &= x_2^{(R,I)}\sqrt{(\Delta \pi_k^{(R,I)})_0^2},\end{aligned} \tag{10}$$

where $x_{1,2}^{(R,I)}$ are random variables, characterized by a Gaussian distribution centered at zero with dispersion equal to 1, $\Delta y_k^{(R,I)}$ and $\Delta \pi_k^{(R,I)}$ are the uncertainties of $y_k^{(R,I)}$ and $\pi_k^{(R,I)}$ respectively in the precollapse state. This is, in a sense, a very simple scheme and one could argue that it represents a natural prescription that treats the field and conjugate momenta on an equal footing. However, a close examination (specifically, a close look at Eq. (2)) indicates that field and momentum conjugate play rather different roles in determining the gravitational perturbation that results after the collapse. There we see that the momentum conjugate is the quantity that determines the Newtonian potential.

This leads us to consider a collapse scheme in which it is only the expectation value of the conjugate momentum the one that changes as a result of the collapse (we would be taking here a view according to which, heuristically speaking, the uncertainty of the source of the metric perturbation, the Newtonian potential, is somehow connected to the triggering of the collapse of the source). See a more detailed discussion of these ideas in [2] and the motivating ideas in [6–9]. Thus we define:

Scheme II: It is the scheme where it is only the expectation value of the conjugated momentum the one that changes as a result of the collapse, and it does so in a random way, dictated by the corresponding uncertainties of the precollapse state, so that, immediately after the collapse time η_k^c, the expectation values are determined by

$$\langle \hat{y}_k^{(R,I)}(\eta_k^c)\rangle_\Omega = 0, \qquad \langle \hat{\pi}_k^{(R,I)}(\eta_k^c)\rangle_\Omega = x^{(R,I)}\sqrt{(\Delta \pi_k^{(R,I)})_0^2}, \tag{11}$$

where $x_{1,2}^{(R,I)}$ are random variables, characterized by a Gaussian distribution centered at zero with dispersion of 1, and $\Delta \pi_k^{(R,I)}$ is the uncertainty of $\pi_k^{(R,I)}$ in the precollapse state.

We should note that an additional and crucial piece of information would be required to determine the primordial spectra: the exact values of the collapse times for each mode. Again, having no knowledge of the physics behind the collapse, all we can do is to assume that whatever that is, it has no intrinsic preferential directionality and thus that $\eta_{\vec{k}}^c$ is only a function of $k = ||\vec{k}||$, but otherwise take that function as unknown. We will then parametrize in simple ways our ignorance about this function and attempt to extract constraints from the data.

There are of course many more possibilities of collapse schemes but we limit our consideration to only those two, because they seem simple and quite natural. Next, we investigate these two schemes in detail at a quantitative level.

IV. COMPARING WITH OBSERVATIONAL DATA

Given the schemes proposed, and after some lengthy algebraic manipulations, one can determine (see Ref. [10]) the functions $C(k)$'s and then use them to compare the resulting predictions for the shape of the spectrum to observations. It was shown in Refs. [2,10] that we can recover the power spectrum of initial fluctuations of the standard cosmological model if $C(k) = 1$. Therefore, the power spectrum of the collapse models can be written as:

$$P(k) = A_s k C(k) \tag{12}$$

where A_s is the amplitude of the scalar fluctuations.

The function $C(k)$ resulting from Eq. (10) for scheme I has the following form:

$$C_{\mathrm{I}}(k) = 1 + \frac{2}{z_k^2}\sin^2\Delta_k + \frac{1}{z_k}\sin(2\Delta_k), \tag{13}$$

whereas the one corresponding to the scheme II is:

$$C_{\mathrm{II}}(k) = 1 + \left(1 - \frac{1}{z_k^2}\right)\sin^2\Delta_k - \frac{1}{z_k}\sin(2\Delta_k), \tag{14}$$

where $z_k \equiv k\eta_k^c$, $\Delta_k = k(\eta_{\mathrm{EI}} - \eta_k^c)$ and η_{EI} refers to the conformal time at the end of the inflationary period.[7] We refer to them hereafter as Model I and Model II, respectively.

In Ref. [10] a preliminary study of these two schemes and one additional scheme was performed. That was a relatively simple analysis concentrating on the main features of the resulting spectrum, but ignoring the late-time physics corresponding to the effects of reheating and acoustic oscillations (represented by $\mathcal{T}(k)$). Thus, the actual comparison with empirical data was not possible except for obtaining order-of-magnitude estimates. A detailed comparison with the very precise data available, requires a much more complex analysis, such as the one we will conduct in this work.

We recall that the standard form of the predicted spectrum is recovered if one replaces $C(k)$ by a constant. We will explore the sensitivity for small deviations of the "z_k independent of k pattern" by considering a linear departure from the situation in which z_k is independent of k. That will be characterized by z_k as $z_k = A + Bk$. This will allow us to examine the robustness of the collapse scheme in as far as predicting the standard spectrum. In such way, the times of collapse for each mode k can also be written in terms of A and B as follows: $\eta_k^c = A/k + B$. We can use this formula to compute the collapse time for the relevant modes we observe in the CMB, namely, those that cover the range of the multipoles of interest, $1 \leq l \leq 2600$. We can made use of the approximate relation[8] $l \sim \pi k R_D$, where R_D is the *comoving* radius of the last scattering surface, in order to interpret heuristically the result of the analysis and to set reasonable viability constraints on the parameters of the model. In standard cosmology[9] it is given by $R_D = \frac{2}{H_0}(1 - \sqrt{a_D})$, where we have normalized the scale factor to be $a_0 = 1$ today, so $a_D \equiv a(\eta_D) \simeq 10^{-3}$, and H_0 is the Hubble constant today. Its numerical value is $R_D = 5816.31h^{-1}$ Mpc. Thus, the relevant modes for the CMB are those in the range 4×10^{-5} Mpc$^{-1} \leq k \leq 0.11$ Mpc^{-1}. The collapse times for these modes can be regarded as the times in which inhomogeneities and anisotropies first emerged at the corresponding scales.

A. Physical meaning of the obtained results

The analysis carried out in previous works on this approach [2,10] does not take into account the evolution of the perturbation beyond the end of inflation and thus their results, even though they provide certain general qualitative and quantitative information about the modifications the general approach leads to, cannot be considered as leading to actual bounds on the parameters extracted from data. In this work we want to extract actual bounds that could, in the future, be taken as clues on the nature of the physics that might lie behind what we represent at the phenomenological level by the collapse mechanism. In particular, we need to ensure that when considering the collapse as being described within the inflationary regime, the times where the relevant collapses occur do indeed fall within that regime. Hence, we will impose *a priori* limits on the values of A and B, so that the collapse of the wave function can occur only at a time between the beginning (t_{BI}) and the end (t_{EI}) of the inflationary epoch. In terms of conformal times:

$$\eta_{\mathrm{BI}} < \eta < \eta_{\mathrm{EI}}. \tag{15}$$

The period of inflationary expansion prior to the radiation dominated era, corresponds to negative conformal time. The initial singularity (or more precisely, the quantum gravity regime) is pushed back into large and negative values of the conformal time and can be pushed arbitrary far depending on the duration of inflation [13].

Now, we estimate the time scales for the beginning and the end of the inflationary epoch. The value of the conformal time at the end of inflation, is determined from the "temperature" of the radiation era viewed as a function of the scale factor: $a(t_0)T(t_0) = a(t_{\mathrm{EI}})T(t_{\mathrm{EI}})$ where t_0 is the present time, $a(t_0) = 1$, t_{EI} is the time at the end of inflation, and $T_0 = 2.728$ K. Taking the usual values for inflationary models, $T(t_{\mathrm{EI}}) \simeq 10^{15}$ GeV, and consequently $a(t_{\mathrm{EI}}) = 2.35 \times 10^{-28}$. We then use the relation between conformal time and scale factor during the inflationary era, $a(\eta) = -\frac{1}{H_I \eta}$, where H_I is the value of the Hubble constant during this epoch. In most inflationary models, H_I can be estimated as: $H_I^2 = \frac{8\pi G}{3}V_I$ where V_I is the inflationary potential. Let us assume that $V_I \simeq 10^{60}$ GeV^4, then we obtain $H_I = 2.37 \times 10^{11}$ GeV and thus

$$\eta_{\mathrm{EI}} = -1.8 \times 10^{16}\ \mathrm{GeV}^{-1} = -7.2 \times 10^{-22}\ \mathrm{Mpc}. \tag{16}$$

We express the results in Mpc because these are the common units for time and length used in Boltzmann codes that

[7]This expression is different from the one in previous papers [2,10], because in those, the work relied on an approximation in which the effects of the plasma physics relevant to the era between the end of inflation and decoupling are ignored.

[8]The relation between the angular scale θ and the multipole l is $\theta \sim \pi/l$. The comoving angular distance, d_A, from us to an object of physical linear size L, is $d_A = L/(a\theta)$. $L/a \sim 1/k$, $d_A = R_D$ if the object is in the LSS, and using the first expression in this footnote, we get $l \sim \pi k R_D$.

[9]In the present work we will be ignoring the effects of the late time acceleration associated with the so called "Dark Energy" as this complication is thought not to impact on the results in any substantial way.

solves the recombination equations, such as CAMB [14]. In order to solve the "horizon" and "flatness" problem, inflationary models require 80 e-folds of inflation:

$$\log\left(\frac{a(t_{\rm EI})}{a(t_{\rm BI})}\right) = H_I(t_{\rm EI} - t_{\rm BI}) = 80. \quad (17)$$

Thus, we obtain: $a(t_{\rm BI}) = 4.24 \times 10^{-63}$, and using the relation between the scale factor and conformal time during inflation, we get:

$$\eta_{\rm BI} = -9.9 \times 10^{50}\ {\rm GeV}^{-1} = -1.6 \times 10^{14}\ {\rm Mpc}. \quad (18)$$

Let us recall now that in the models that are being studied, each mode is thought to collapse at a different time given by

$$\eta_k^c = \frac{A}{k} + B, \quad (19)$$

where A and B are constants. Therefore, for the collapse of the wave function to occur during the inflationary period, the values of A and B should satisfy the following relation for all values of k:

$$\eta_{\rm BI} - \frac{A}{k} < B < \eta_{\rm EI} - \frac{A}{k}. \quad (20)$$

Demanding that these inequalities hold for all the relevant modes, leads to the desired *a priori* bounds on the model parameters.

B. Characteristic signatures of the models on the CMB fluctuation spectrum

In order to analyze the effects on the CMB fluctuations power spectrum, let us first define the fiducial model, which will be taken just as a reference to discuss the results we obtain for the collapse models. The fiducial model is a ΛCDM model with the following cosmological parameters: baryon density in units of the critical density, $\Omega_B h^2 = 0.02247$; dark matter density in units of the critical density, $\Omega_{\rm CDM} h^2 = 0.1161$; Hubble constant in units of ${\rm Mpc}^{-1}\ {\rm km\,s}^{-1}$, $H_0 = 68.7$; reionization optical depth, $\tau = 0.088$; and the scalar spectral index, $n_s = 0.959$. These are the best-fit values presented by the WMAP collaboration using the final 7-year release data [15] and the power spectrum from Sloan Digital Sky Survery DR7 LRG [16].

Figures 1, 2, 5, and 6, show the prediction for the temperature fluctuation spectrum for Models I and II for various values of the parameters A and B. The value of χ^2 in the figures is calculated using both temperature and temperature-polarization fluctuation data from WMAP 7-year release. We can see that the different collapse models have distinct effects on the CMB temperature fluctuation spectrum, and furthermore, that these effects depend rather strongly on the values of the parameters A and B which determine the collapse times of the various modes.

Let us first analyze the case of Model I: When fixing $A = -10$ or $A = -10^{-4}$, we find that there is no change within the range of B studied here (with respect to the fiducial model) in the position of the Doppler peaks or in the height of the first peak. On the other hand, we note an increase in the height of the secondary peaks, with the amplitude depending on the value of the free parameter B. Next, we set $A = -10^8$ (see Fig. 1, right panel); in this case there is no change in the first peak (with respect to the fiducial model), while there is a extremely small increase in the height of the second peak and a a similar decrease in the height of the third peak. In fact one does not observe any important change in the spectrum for different values of B (other values of B in the explored range give the same spectrum). The small difference between the spectrum of the collapse models and the fiducial model is due to the fact that the former uses the canonical value for the spectral index ($n_s = 1$) while the latter is the best fit value to the data found by the WMAP collaboration assuming the

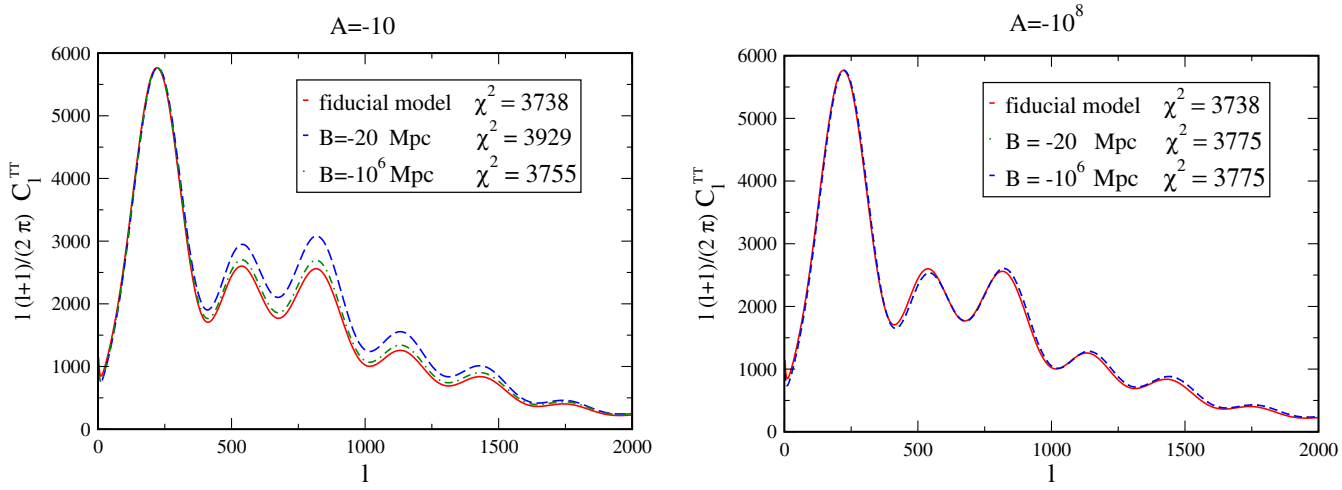

FIG. 1 (color online). The temperature autocorrelation (TT) power spectrum for Model I (Left: $A = -10$, Right: $A = -10^8$). All models are normalized to the maximum of the first peak of the fiducial model. The value of χ^2 is calculated using only WMAP 7-year release data. The solid line corresponds to the fiducial model.

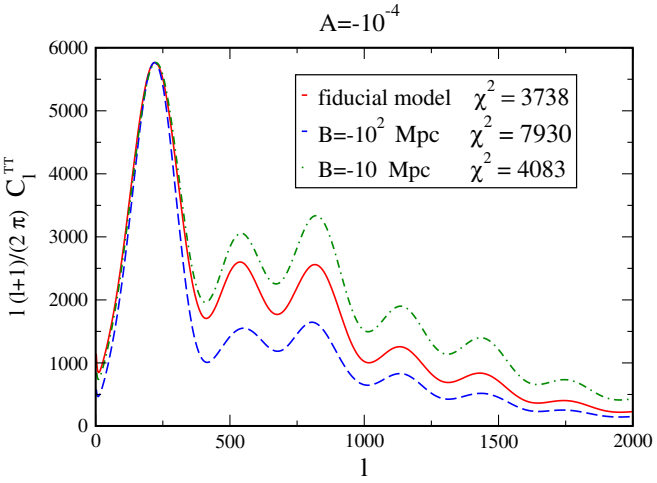

FIG. 2 (color online). The temperature autocorrelation (TT) power spectrum for Model I ($A = -10^{-4}$). All models are normalized to the maximum of the first peak of the fiducial model. The value of χ^2 is calculated using only WMAP 7-year release data (both temperature and temperature-polarization power spectrum are included). The solid line corresponds to the fiducial model.

standard cosmological model (which differs slightly from 1). We have also studied the results for other various large negative values of A (not shown here) and found that the behavior is similar to that of the case $A = -10^8$. This is the result of a simple preliminary analysis; the exact value of A at which the behavior of the CMB spectrum changes becomes important, phenomenologically speaking, will be determined from the statistical analysis (see Section V). As the most accurate observational data corresponds to the first peak, it is expected that the collapse Model I with large values of A will be phenomenologically indistinguishable from the fiducial model, as seen in Fig. 1 (right panel). Indeed, the difference in the value of the quality-of-fit estimator χ^2, is found to be not significant within 1σ.

Figures 3 and 4 show the prediction for the temperature-polarization cross-power spectrum for Model I. Here again, the models with $A = -10^8$ differ very little from the fiducial model and show no relevant dependence of the results on values of B within the explored range. Regarding the cases of $A = -10$ and $A = -10^{-4}$, we find (in comparison with the fiducial model) an increase in the values of the secondary peaks and a decrease in the amplitude of the valleys, but the relative change is less relevant than that in the temperature fluctuation power spectrum.

Let us now focus on Model II (see Fig. 5). Here again, the effect is different for different values of A: Considering firstly the case of $A = -10$, we find that there is a shift in the position of the peaks, and in one case ($B = -10^3$), the first peak is replaced by two peaks. On the other hand, when setting $A = -10^8$ or $A = -10^{-4}$, we find generically a shift in the position of the first peak. In both cases, there is also a change in the height of the secondary peaks, with the magnitude of the change depending on the values of A and B. Figures 7 and 8 show the prediction for the temperature-polarization cross-power spectrum for Model II. Here again, we observe (in comparison with the fiducial model) an increase in the value of the peaks and a decrease in the values at the valleys for all cases, with the magnitude of the changes depending on the value of B. Therefore, in this case, collapse models can be clearly distinguished from the fiducial model. The difference in behavior of the two models can be understood by looking at Eqs. (13) and (14): for sufficiently large values of A and/or B, $C_1(k)$ becomes independent from k, while the second term of $C_2(k)$ does not vanish in the limit of large values of $k\eta_k^c$. We would like to emphasize the importance of this preliminary analysis on the behavior of the collapse

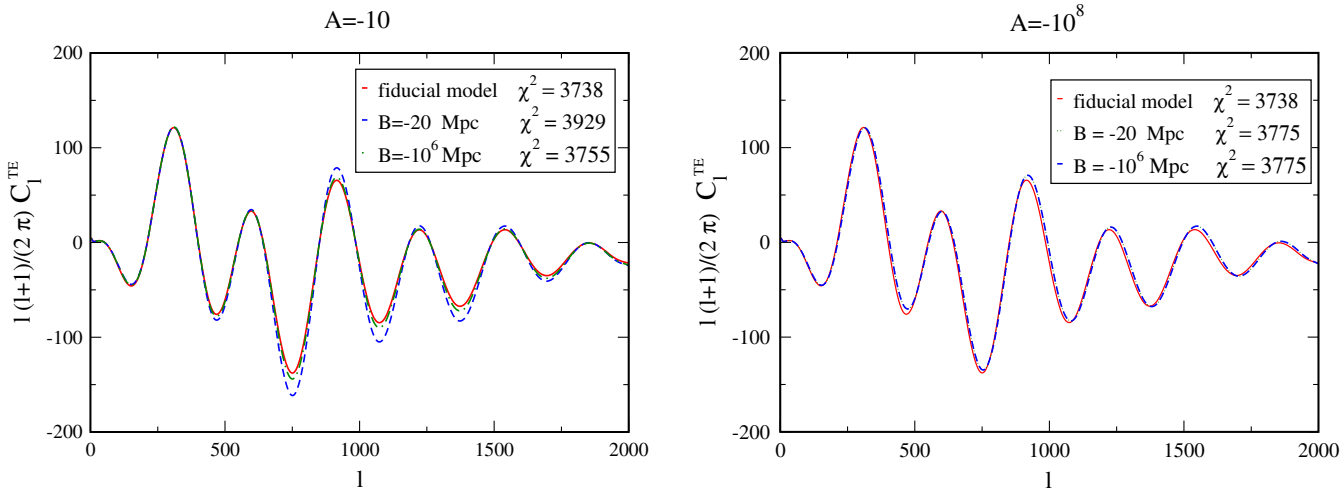

FIG. 3 (color online). The temperature-polarization (TE) cross-power spectrum for Model I (Left: $A = -10$, Right: $A = -10^8$). All models are normalized to the maximum of the first peak of the fiducial model. The value of χ^2 is calculated using only WMAP 7-year release data (both temperature and temperature-polarization power spectrum are included). The solid line corresponds to the fiducial model.

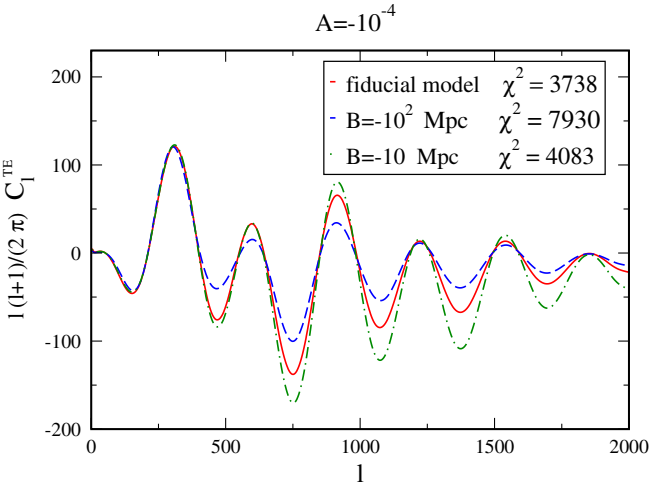

FIG. 4 (color online). The temperature-polarization (TE) cross-power spectrum for Model I ($A = -10^{-4}$). All models are normalized to the maximum of the first peak of the fiducial model. The value of χ^2 is calculated using only WMAP 7-year release data (both temperature and temperature-polarization power spectrum are included). The solid line corresponds to the fiducial model.

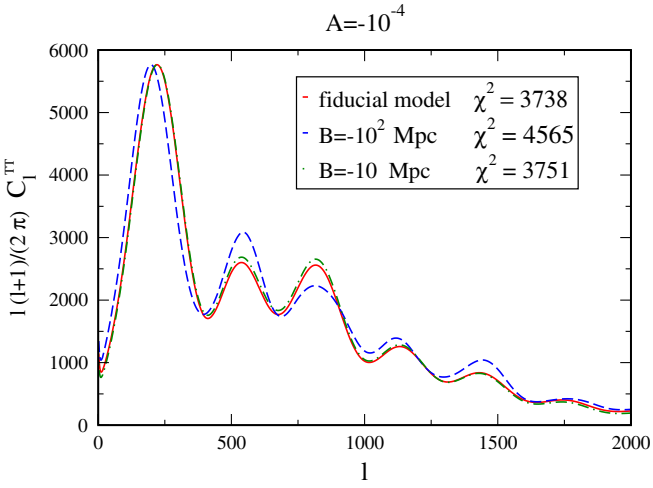

FIG. 6 (color online). The temperature autocorrelation (TT) power spectrum for Model II ($A = -10^{-4}$). All models are normalized to the maximum of the first peak of the fiducial model. The value of χ^2 is calculated using only WMAP 7-year release data (both temperature and temperature-polarization power spectrum are included). The solid line corresponds to the fiducial model.

schemes, to determine the appropriate method for the statistical analysis to explore the various relevant regions of parameter space, as we described in detail in Sec. V.

V. RESULTS

The observational data used for the analysis are the temperature and temperature-polarization power spectra obtained from the final WMAP 7-year release [15], and other CMB experiments such as CBI [17], ACBAR [18], BOOMERANG [19,20], BICEP [21] and QUAD [22], together with the matter power spectrum traced by LRGs as measured in the Sloan Digital Sky Survey DR7 [16]. We consider a spatially-flat cosmological model with adiabatic density fluctuations, in which we add the effect of the collapse models in the power spectrum of the initial fluctuations. The parameters allowed to vary are:

$$P = (\Omega_B h^2, \Omega_{\rm CDM} h^2, \Theta, \tau, A_s, A, B), \qquad (21)$$

where Θ is the ratio of the comoving sound horizon at decoupling to the angular diameter distance to the surface of last scattering, τ is the reionization optical depth, A_s is the amplitude of the primordial density fluctuations, and A and B are the model parameters related to the conformal time of collapse of each mode (see Eq. (19)). Given that the

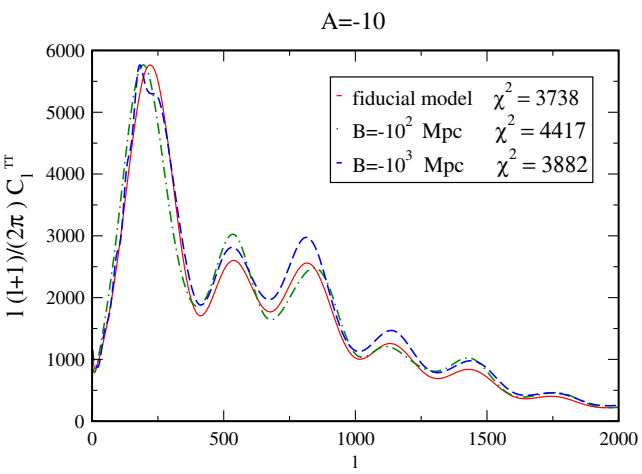

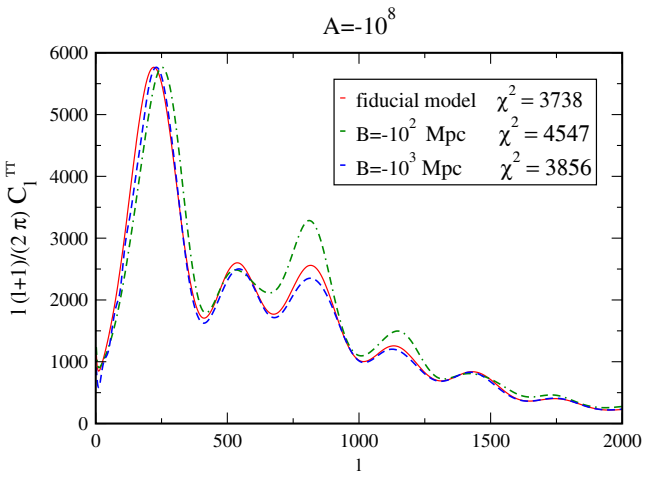

FIG. 5 (color online). The temperature autocorrelation (TT) power spectrum for Model II (Left: $A = -10$, Right: $A = -10^8$). All models are normalized to the maximum of the first peak of the fiducial model. The value of χ^2 is calculated using only WMAP 7-year release data (both temperature and temperature-polarization power spectrum are included). The solid line corresponds to the fiducial model.

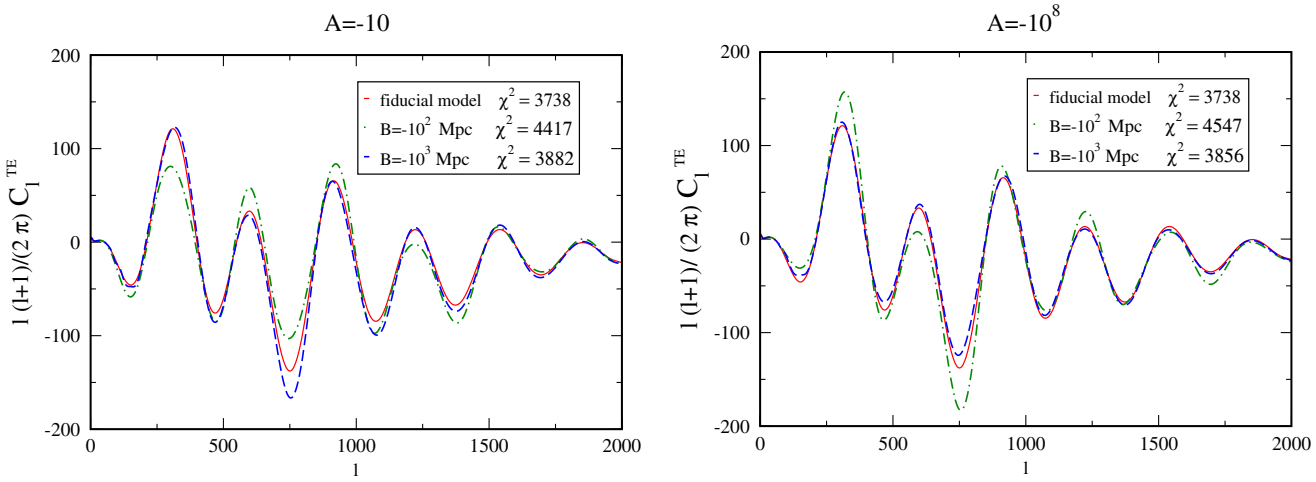

FIG. 7 (color online). The temperature-polarization (TE) cross-power spectrum for Model II (Left: $A = -10$, Right: $A = -10^8$). All models are normalized to the maximum of the first peak of the fiducial model. The value of χ^2 is calculated using only WMAP 7-year release data (both temperature and temperature-polarization power spectrum are included). The solid line corresponds to the fiducial model.

primordial power spectrum of density fluctuations for the collapse models was computed only for the scale invariant case [2,10], the scalar spectral index of density fluctuations (n_s) is fixed to 1 in this paper. However, we should keep in mind that the collapse models allow different values for n_s and the corresponding power spectrum will be studied in future works.

In order to place constraints on the parameters of the quantum collapse models, we modified the primordial power spectrum according to the schemes described in Sec. II. We performed our statistical analysis by exploring the parameter space with Monte Carlo Markov chains

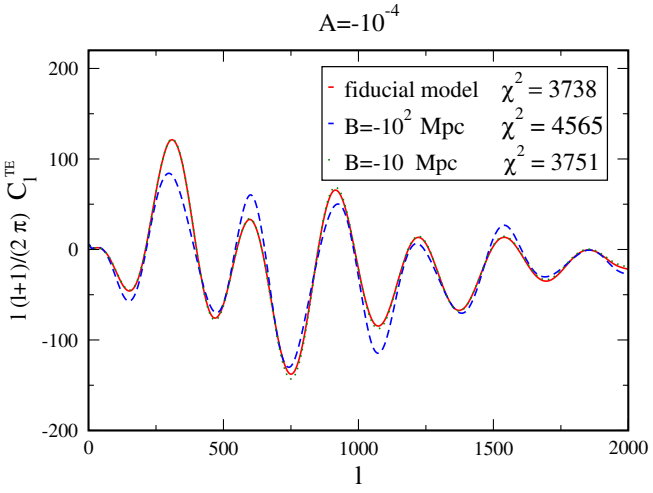

FIG. 8 (color online). The temperature-polarization (TE) cross-power spectrum for Model II ($A = -10^{-4}$). All models are normalized to the maximum of the first peak of the fiducial model. The value of χ^2 is calculated using only WMAP 7-year release data (both temperature and temperature-polarization power spectrum are included). The solid line corresponds to the fiducial model.

generated with the publicly available CosmoMC code of Ref. [23] which uses the Boltzmann code CAMB [14] to compute the CMB power spectra.

In a first trial, we performed the statistical analysis without imposing any prior on the baryon density and found that the confidence interval obtained for $\Omega_B h^2$ turned out to be very large compared to the one obtained by the WMAP collaboration (i.e. without considering the collapse scheme). Therefore, we introduced a gaussian prior on the baryon density, using an independent data, namely, the Big Bang Nucleosynthesis (BBN) bound [24,25].

Initially, we intended to perform the statistical analysis allowing the two parameters of the model, A and B, to vary independently. However, after the first runs we realized that for a very large range of values of A, there was always a range of values of B providing a good fit to the data. Furthermore, in order to allow the Markov chains to explore various orders of magnitude in those parameters, we used the following reparametrization: $a = \sinh(A)$ and $b = \sinh(B)$ (another possible reparametrization is $a = \log(A)$ and $b = \log(B)$, but we are interested in exploring both positive and negative values of A and B). We found that the Markov chains did not converge when both a and b were allowed to vary independently. The reason for this is simply the fact that there are several maxima of the probability function in the parameter space, but the method of Markov chains does not allow to explore all maxima at the same time. In contrast, we found that when we fixed values of A within a rather large range of values, convergence of the Markov chains is found. Moreover, let us recall that the primordial power spectrum in collapse models is a function of $z_k = A + Bk$; by taking $B = 0$, we recover the spectrum corresponding to the standard ΛCDM model with spectral index $n_s = 1$, up to an overall normalization factor. Thus, the parameter B gives a measure of the departure of the

primordial power spectrum with respect to that of the standard model, while phenomenologically A behaves as a normalization factor that is degenerated with A_s. We should note, however, that although the effect on the spectrum of A and A_s is very closely connected, their physical interpretation is quite different. The results of the statistical analysis, for fixed values of A are shown in Tables I, II, and III for collapse models I and II.

Within Model I, a preliminary analysis of the modifications of the CMB fluctuation power spectrum associated with the collapse models indicates that for large values of the parameter A, there is no dependence on the value of B, and also that there is a very small difference between those models and the fiducial one. This last feature is related to the fact that the fiducial model involves a different value of the spectral index n_s (see discussion in Section IV B). These results are, indeed, reflected in the statistical analyses by the fact that for $|A| < 20$, nontrivial bounds on B can be found, while for larger values of A, any value of B gives a good fit to the data. Furthermore, the values of the corresponding cosmological parameters obtained from the statistical analyses for models with $|A| > 20$ is within the 1σ bounds established by the standard analysis of WMAP collaboration made without considering the collapse scheme. In order to confirm the persistence of this behavior, we have explored a large range of A values, from -10^9 to 10^9, changing this value in each step by one order of magnitude, and found results consistent with the previous conclusion. In Table I we show the bounds on B obtained for fixed values of $|A| < 20$ for Model I.

A similar analysis performed for Model II, shows that we should not expect the same behavior as the one obtained for Model I. Indeed, Fig. 5 shows (for two different values

TABLE I. Model I. Mean values and 1σ error for $b = \sinh B$ considering different fixed values of parameter A. The χ^2 estimator is computed for the whole data set. For the fiducial model, $\chi^2_{\rm min} = 3909$. Column 4 refers to the viability of the model (collapse times happen during inflation), and column 5 shows whether there is any restriction to the viability in the range shown by column 2.

A	Mean value and 1σ error	$\chi^2_{\rm min}$	Viability	Restricted
-17.5	$2.74^{+0.28}_{-0.29}$	3910	Y	N
-15	-3.11 ± 0.19	3909	Y	N
-12.5	-2.40 ± 0.36	3910	Y	N
-10	$-0.87^{+0.79}_{-0.74}$	3915	Y	N
-7.5	$1.83^{+0.46}_{-0.38}$	3911	Y	N
-5	$1.95^{+0.24}_{-0.22}$	3909	Y	N
-2.5	$-1.56^{+0.23}_{-0.14}$	3907	Y	N
-1	1.65 ± 0.24	3908	Y	N
-10^{-1}	$0.48^{+0.50}_{-0.51}$	3915	Y	N
-10^{-2}	0.03 ± 0.55	3916	Y	Y
-10^{-3}	0.005 ± 0.54	3916	Y	Y
-10^{-4}	$0.02^{+0.54}_{-0.55}$	3916	Y	Y
10^{-8}	$-0.006^{+0.54}_{-0.55}$	3916	Y	Y
10^{-7}	$0.0005^{+0.56}_{-0.57}$	3916	Y	Y
10^{-6}	-0.016 ± 0.56	3916	Y	Y
10^{-5}	$-0.006^{+0.54}_{-0.55}$	3916	Y	Y
10^{-4}	$0.72 \times 10^{-4} \pm 0.55$	3916	N	-
10^{-3}	$-0.01^{+0.51}_{-0.56}$	3916	N	-
10^{-2}	$-0.05^{+0.54}_{-0.65}$	3916	N	-
10^{-1}	$0.48^{+0.50}_{-0.51}$	3915	N	-
1	-1.68 ± 0.23	3908	N	-
10	$0.81^{+0.74}_{-0.79}$	3915	N	-
12.5	$2.44^{+0.34}_{-0.35}$	3910	N	-
15	$-3.20^{+0.15}_{-0.19}$	3910	N	-
17.5	$2.72^{+0.28}_{-0.30}$	3910	N	-

TABLE II. Model II. Mean values and 1σ error for $b = \sinh B$ considering different fixed negative values of parameter A. χ^2 is calculated for the whole data set. For the fiducial model, $\chi^2_{\rm min} = 3909$. Column 4 refers to the viability of the model (collapse times happen during inflation), and column 5 shows whether there is any restriction to the viability in the range shown by column 2.

A	Mean value and 1σ error	$\chi^2_{\rm min}$	Viability	Restricted
-10^9	1.55 ± 0.30	3908	Y	N
-7×10^8	1.54 ± 0.21	3908	Y	N
-3×10^8	-1.56 ± 0.30	3909	Y	N
-10^8	$-1.64^{+0.21}_{-0.22}$	3908	Y	N
-10^7	$-1.55^{+0.30}_{-0.29}$	3909	Y	N
-10^6	$-1.44^{+0.31}_{-0.30}$	3910	Y	N
-5×10^5	1.78 ± 0.21	3911	Y	N
-10^5	-0.17 ± 0.46	3916	Y	N
-5×10^4	-1.99 ± 0.20	3908	Y	N
-10^4	1.36 ± 0.23	3908	Y	N
-10^3	1.49 ± 0.23	3908	Y	N
-500	1.57 ± 0.30	3908	Y	N
-300	-2.00 ± 0.20	3911	Y	N
-300	1.96 ± 0.20	3911	Y	N
-100	-1.58 ± 0.28	3908	Y	N
-80	$-2.08^{+0.13}_{-0.18}$	3913	Y	N
-50	-1.15 ± 0.34	3913	Y	N
-30	$-1.79^{+0.21}_{-0.20}$	3909	Y	N
-10	1.47 ± 0.26	3908	Y	N
-5	-1.58 ± 0.20	3908	Y	N
-1	-2.01 ± 0.21	3909	Y	N
-10^{-1}	$-2.22^{+0.76}_{-0.65}$	3915	Y	N
-10^{-1}	$2.03^{+1.05}_{-0.84}$	3914	Y	Y
-10^{-2}	$-2.09^{+0.97}_{-0.76}$	3914	Y	N
-10^{-2}	$2.14^{+0.73}_{-0.93}$	3914	N	-
-10^{-3}	$-2.12^{+0.93}_{-0.74}$	3914	Y	N
-10^{-3}	$2.11^{+0.75}_{-0.97}$	3914	N	-
-10^{-4}	$-2.13^{+0.92}_{-0.73}$	3914	Y	N
-10^{-4}	$2.14^{+0.72}_{-0.92}$	3914	N	-

TABLE III. Model II. Mean values and 1σ error for $b = \sinh B$ considering different fixed positive values of parameter A. χ^2 is calculated for the whole data set. For the fiducial model, $\chi^2_{\rm min} = 3909$. Column 4 refers to the viability of the model (collapse times happen during inflation), and column 5 shows whether there is any restriction to the viability in the range shown by column 2.

A	Mean value and 1σ error	$\chi^2_{\rm min}$	Viability	Restricted
10^{-8}	$-2.09^{+0.96}_{-0.76}$	3914	Y	N
10^{-8}	$2.14^{+0.71}_{-0.90}$	3914	N	-
10^{-7}	$-2.06^{+0.97}_{-0.77}$	3914	Y	N
10^{-7}	$2.10^{+0.96}_{-0.75}$	3914	N	-
10^{-6}	$-2.09^{+1.00}_{-0.77}$	3914	Y	N
10^{-6}	$2.12^{+0.76}_{-0.97}$	3914	N	-
10^{-5}	$-2.00^{+1.05}_{-0.81}$	3914	Y	N
10^{-5}	$2.14^{+0.72}_{-0.90}$	3914	N	-
10^{-4}	$-2.14^{+0.87}_{-0.71}$	3914	N	-
10^{-4}	$2.11^{+0.75}_{-0.98}$	3914	N	-
10^{-3}	$-2.12^{+0.93}_{-0.74}$	3914	N	-
10^{-3}	$2.11^{+0.95}_{-0.74}$	3914	N	-
10^{-2}	$-2.12^{+0.95}_{-0.75}$	3914	N	-
10^{-2}	$2.15^{+0.73}_{-0.95}$	3914	N	-
10^{-1}	$-2.43^{+0.57}_{-0.51}$	3915	N	-
10^{-1}	$0.00^{+0.75}_{-0.76}$	3915	N	-
10^{-1}	$2.42^{+0.47}_{-0.51}$	3914	N	-
10	-1.47 ± 0.25	3908	N	-
100	1.58 ± 0.27	3908	N	-
10^3	1.50 ± 0.22	3908	N	-
10^4	$-1.33^{+0.32}_{-0.34}$	3911	N	-
10^5	$0.19^{+0.44}_{-0.46}$	3916	N	-
10^6	$1.46^{+0.29}_{-0.30}$	3910	N	-
10^7	1.53 ± 0.31	3909	N	-
10^8	1.65 ± 0.21	3908	N	-
10^9	$-1.53^{+0.29}_{-0.30}$	3908	N	-

of A) that the prediction of Model II on the C_ℓ's depends rather strongly on the value of B. Results from the statistical analysis for fixed values of A are shown in Table II and III.

As mentioned previously in this section, we could not perform a statistical analysis with A and B varying jointly as free parameters, due to the fact that there are several maxima of the probability function. Indeed, Tables II and III show that, for several values of A, we obtain two different maxima for which the difference between the value of $\chi^2_{\rm min}$ does not exceed the value of 1 and thus one cannot discriminate between them. There is even one case ($A = 0.1$) in Model II (see Table III) in which there are three maxima. However, we should emphasize an important difference between the statistical analysis performed for $A = -300$ in Model II and the ones corresponding to the other values mentioned above. In the first case, we have performed two different statistical analyses with different initial values of $b = \sinh(B)$ when running COSMOMC and obtained convergence of the Markov chains to one maximum at each time. The values of the errors have been calculated with the GETDIST program, as is usually done in this kind of analyses. On the other hand, for values of $|A| < 1$, we have performed one statistical analysis for each value of A and obtained a marginalized likelihood with two peaks, for the parameter B. We have tried to change the initial value of $b = \sinh(B)$ in order to obtain convergence to a single value at the time, with no success. As the GETDIST program determines the confidence interval assuming that there is just one maximum of the likelihood function, we need some alternative method to calculate those. We have thus computed the confidence interval for values of $|A| < 1$ in Model II by estimating the limits of integration for which the integral of the marginalized likelihood function yields 68% of the value of the same integral over that peak. Therefore, it is not surprising that the 1σ errors calculated for $A < 1$ are 4 times larger than those calculated by the GETDIST program.

Next, let us recall the discussion of Sec. IV A where for a given value of A, we calculated the corresponding range of values of B that ensure that the time of collapse for the mode k occurs during the inflationary period. Then, by considering the values of A for which the collapse schemes are tested (see Tables I, II, and III), Eq. (20) implies that for $A > 0$ we must have $B < -\frac{A}{k_{\rm min}}$ and that for $A < 0$ the condition is $B < -\frac{A}{k_{\rm max}}$. Therefore, we have added the dotted line corresponding to $B = -\frac{A}{k_{\rm max}}$ in Figs. 9 and 11 and the dotted line corresponding to $B = -\frac{A}{k_{\rm min}}$ in Fig. 10 and 12 above which the solutions found are nonphysical and thus excluded. It should be noted that there are some cases where only parts of the solution are physically viable. In order to facilitate this discussion we have added column 4 in Tables I, II, and III which indicates if the model is viable or not, and column 5 in the same tables indicates the cases where there is a further restriction on the range of values of B for the viability of the solution. In the rest of this section we will discuss only those results that are relevant for our model, and exclude those nonviable values mentioned in the above paragraph. Recall that, unfortunately, and as it has been already mentioned, the present analysis does not allow us to determine any possible degeneration, as far as the fit is concerned, between the model parameters A and B. However, from Fig. 9 we can see that the allowed values of B—within 1σ error- for $A > -20$ turn out to lie in the range $|\sinh(B)| < 3.2$ for Model I; recall that for $A < -20$, the resulting CMB spectrum is the same for all values of B and very similar to the fiducial model and therefore, any value of B among those tested in this paper ($B = -10^9 \cdots 10^9$)) provides a good fit to the data. On the other hand, for Model II, the allowed values of B—within 1σ error- lie in the range $|\sinh(B)| < 3$ for Model II for all values of A studied in this paper. This

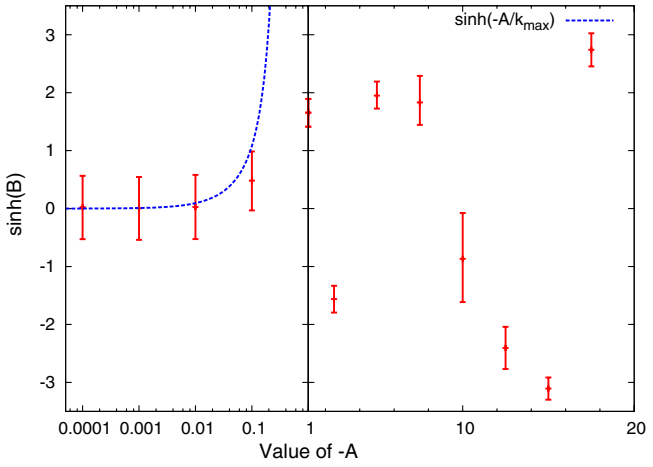

FIG. 9 (color online). Results for Model I: Bounds on $b = \sinh(B)$ obtained for fixed negative values of A. The area below the dotted line $\sinh(B) < \sinh(-\frac{A}{k_{\max}})$ indicates the region where the collapse of all modes happens during the inflationary period.

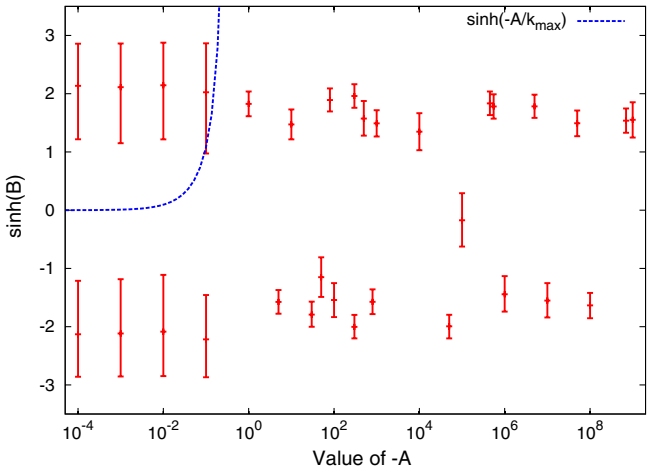

FIG. 11 (color online). Results for Model II: Bounds on $b = \sinh(B)$ obtained for fixed negative values of A. The area below the dotted line $\sinh(B) < \sinh(\frac{-A}{k_{\max}})$ indicates the region where the collapse of all modes happens during the inflationary period.

allows us to set the bounds $B < 1.88$ Mpc for $A < -20$ in Model I, and $B < 1.81$ Mpc for Model II. On the other hand, it is also interesting to note that for all the studied cases with $|A| < 1$ in Model I, the confidence interval includes the case $B = 0$ with a maximal allowed departure from that value of 0.6. In contrast, for the cases $|A| > 1$ in Model I and for almost all cases considered in Model II, the value $B = 0$ is excluded within 2σ, except for the case $A = -10^5$ for Model II and $A = 10$ for Model I.

The results of the statistical analysis for the cosmological parameters are shown in Figs. 13–16 for Models I and II. We can distinguish two behaviors: i) Model I with $-20 < A < -1$; Model II with $A < -1$; ii) Models I with $|A| < 1$; Model II with $|A| < 1$. Let us remind that for $|A| > 20$ in Model I we recover the scale-invariant HZ spectrum and therefore the constraints on the cosmological parameters are those estimated by the WMAP collaboration [15]. For models included in case i), most of the estimated values for the cosmological parameters within the collapse models are in agreement with those obtained by the WMAP collaboration using the 7-year data release and considering a standard ΛCDM model. The values obtained for Θ are marginally consistent with those obtained by the WMAP collaboration. However, there is a better agreement in the results obtained for H_0, which is derived from Θ and other cosmological parameters. Let us now discuss some exceptions. For the case $A = -10$ in Model I, the values obtained for $\Omega_b h^2$ and H_0 are at

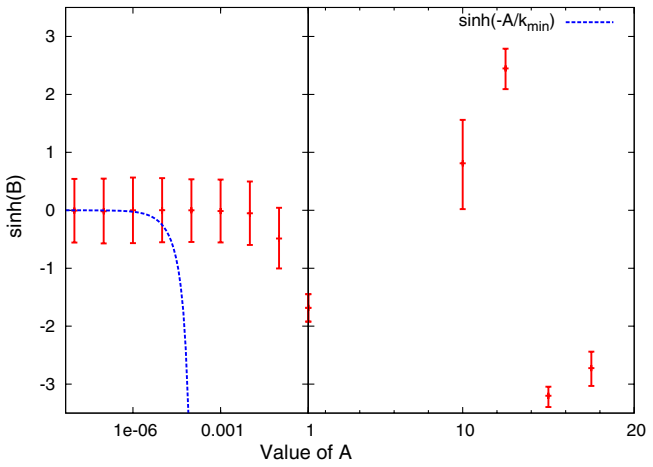

FIG. 10 (color online). Results for Model I: Bounds on $b = \sinh(B)$ obtained for fixed positive values of A. The area below the dotted line $\sinh(B) < \sinh(-\frac{A}{k_{\min}})$ indicates the region where the collapse of all modes happens during the inflationary period.

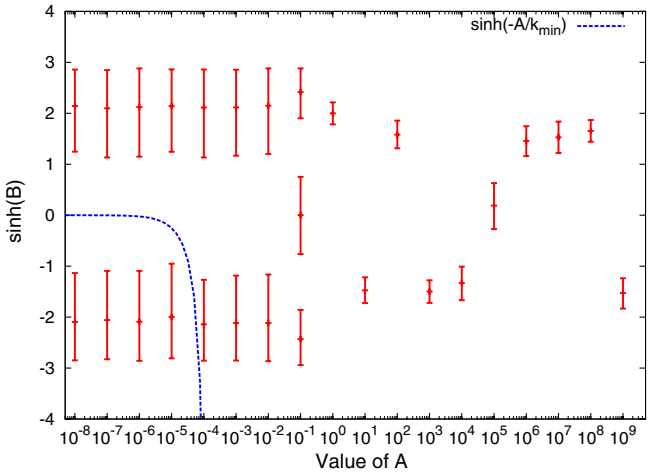

FIG. 12 (color online). Results for Model II: Bounds on $b = \sinh B$ obtained for fixed positive values of A. The area below the dotted line $\sinh(B) < \sinh(-\frac{A}{k_{\min}})$ indicates the region where the collapse of all modes happens during the inflationary period.

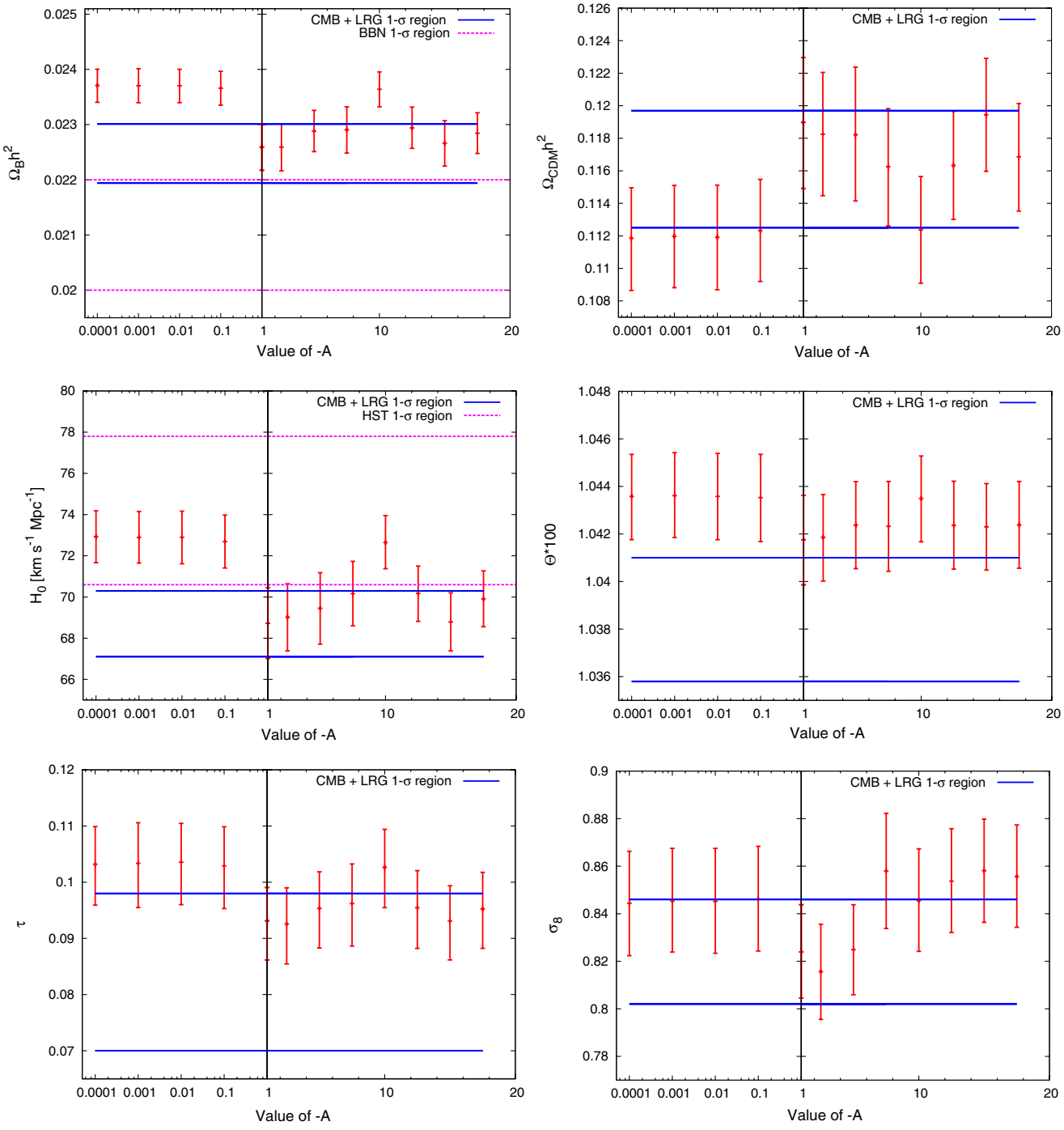

FIG. 13 (color online). Results for Model I: Best-fit parameter values and 1σ errors for the cosmological parameters obtained for fixed negative values of A. Comparison with the values obtained by the WMAP collaboration (and other data sets, where relevant), is also shown. For convenience, the value of $-A$ is plotted in the x-axis. Values of $-20 < A < -1$ belong to case i) described in the text, while values of $|A| < 1$ correspond to case ii).

variance with the values obtained by the WMAP collaboration within 2σ, while there is agreement within 3σ. For the case $A = -10^5$ in Model II, the values obtained for $\Omega_b h^2$ and H_0 are at variance with the values obtained by the WMAP collaboration within 1σ, while there is an agreement within 2σ. On the other hand, it is important to discuss consistency of our results with independent data such as the baryon density inferred from BBN [24,25][10] and the constraint on the Hubble constant presented in Ref. [26]. It should be noted that the 1σ BBN region for $\Omega_b h^2$ shown in Figs. 13–16 refers to the constraint

[10]Recall that have put a gaussian prior on the baryon density using constraints inferred from BBN.

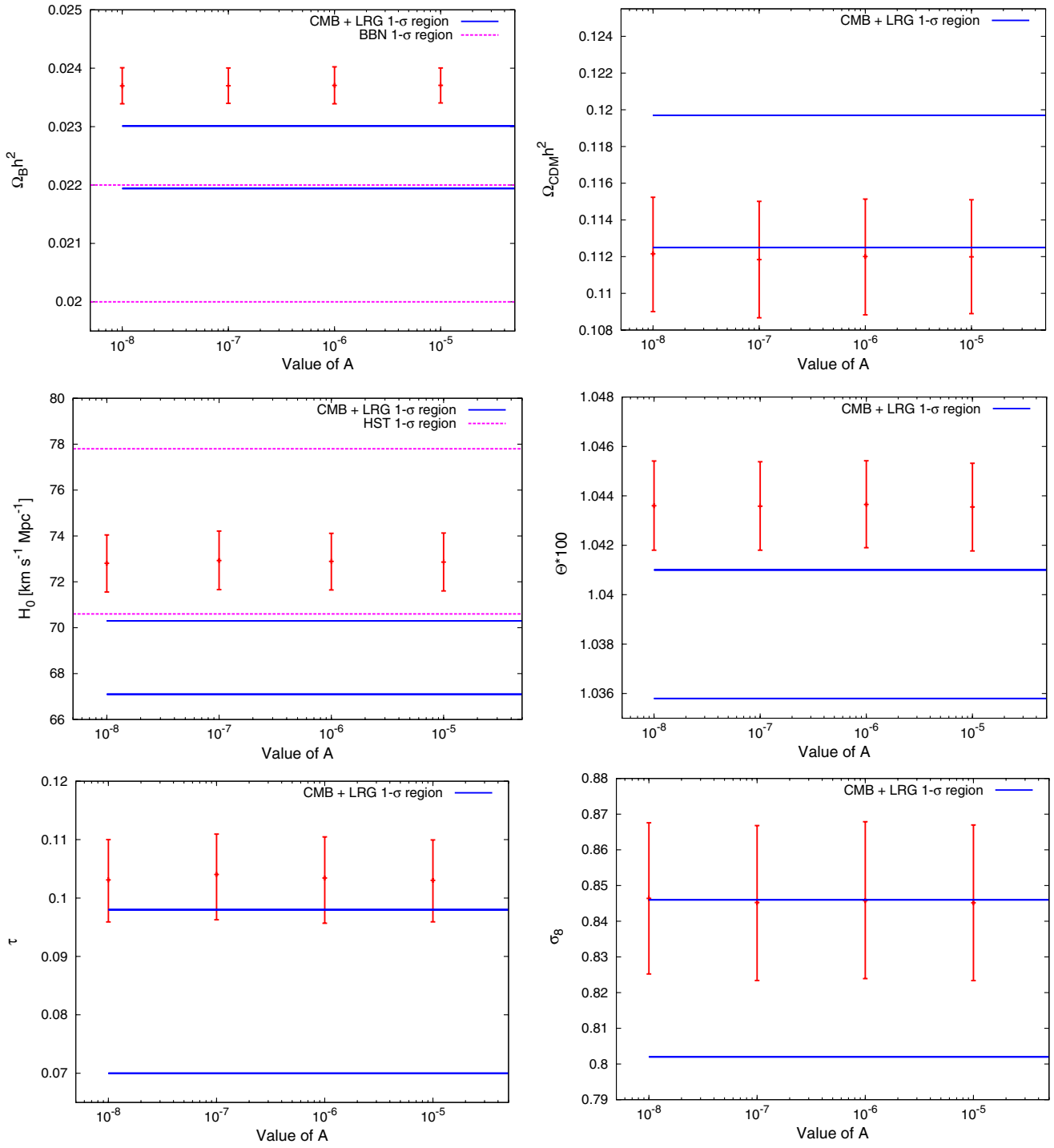

FIG. 14 (color online). Results for Model I: Best-fit parameter values and 1σ errors for the cosmological parameters obtained for fixed positive values of A. Comparison with the values obtained by the WMAP collaboration (and other data sets, where relevant), is also shown. All of these values correspond to case ii) described in the text.

obtained using the observational abundances of deuterium, which is the most stringent one. However, one should keep in mind that by considering the ^{4}He abundance, the constraint on the baryon density softens substantially, and in fact it leads to a region which is consistent with the constraint obtained with the CMB data. Indeed, the values we obtained for $\Omega_b h^2$ are marginally consistent with the value inferred from deuterium abundance BBN constraints within 1σ, while there is full consistency with value inferred from the primordial abundance of ^{4}He. On the other hand, the values of H_0 obtained in our study are marginally consistent with the

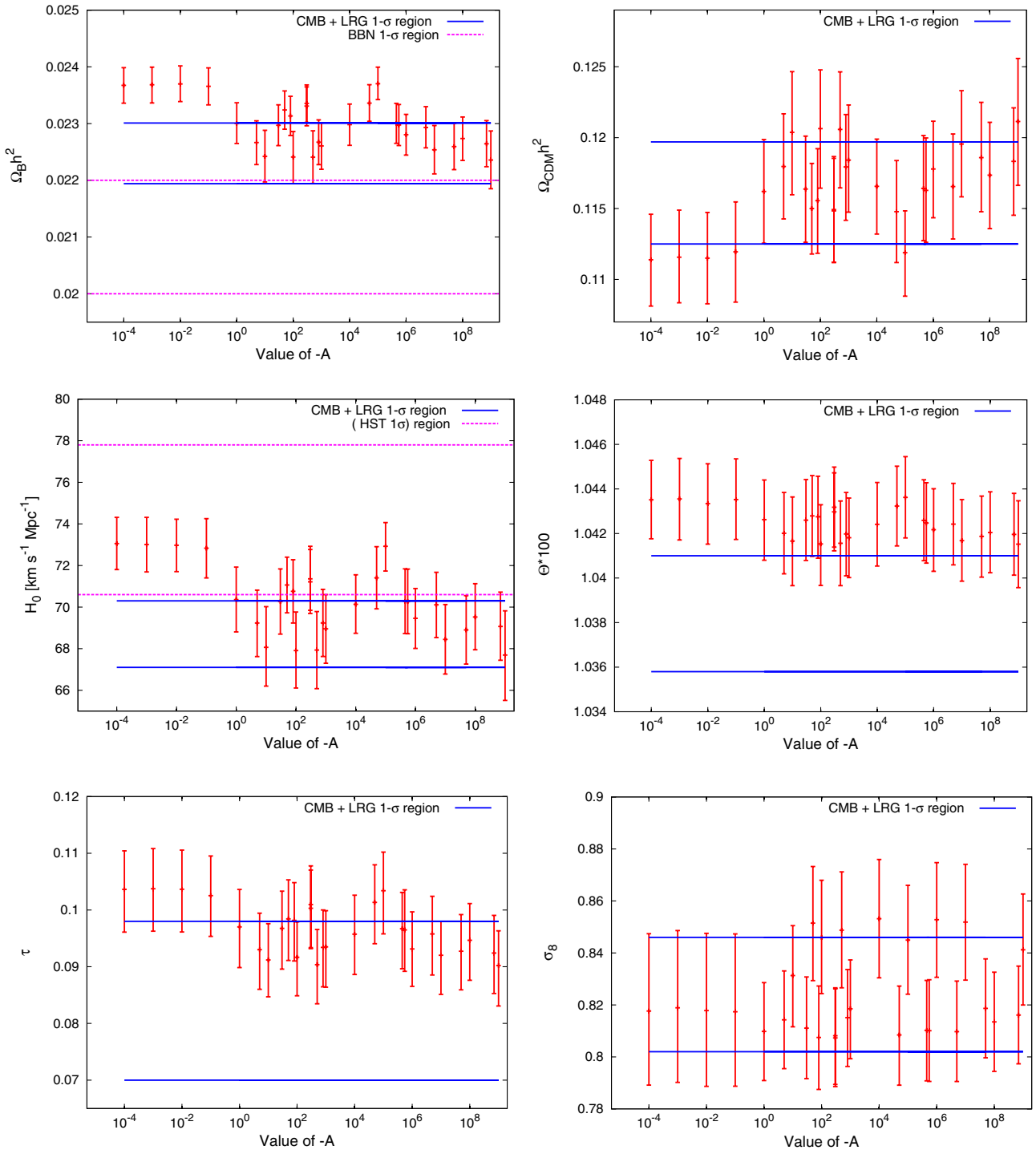

FIG. 15 (color online). Results for Model II: Best-fit parameter values and 1σ errors for the cosmological parameters obtained for fixed negative values of A. Comparison with the values obtained by the WMAP collaboration (and other data sets, where relevant), is also shown. For convenience, the value of $-A$ is plotted in the x-axis. Values of $|A| > 1$ belong to case i) described in the text, while values of $|A| < 1$ correspond to case ii).

constraint extracted from Hubble Space Telescope (HST) data.

Let us now discuss models included in case ii). The values of $\Omega_b h^2$ obtained are consistent with the values obtained by the WMAP collaboration in the context of the standard cosmological model within 2σ. On the other hand, there is disagreement with the deuterium inferred BBN constraint on $\Omega_b h^2$ within 3σ, while there is consistency with the value inferred from the ^{4}He abundance. The values of H_0 obtained are at variance with the ones

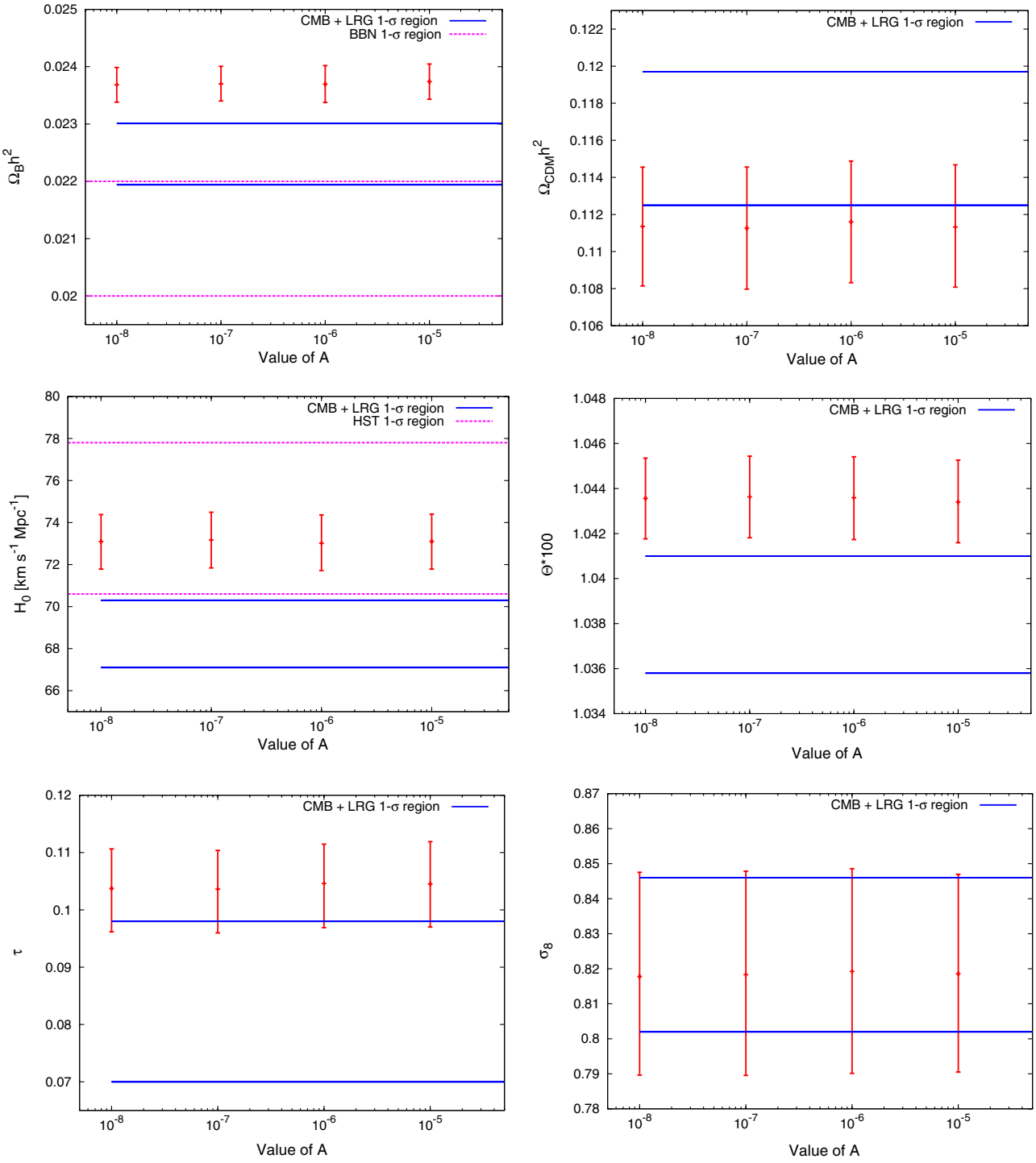

FIG. 16 (color online). Results for Model II: Best-fit parameter values and 1σ errors for the cosmological parameters obtained for fixed positive values of A. Comparison with the values obtained by the WMAP collaboration (and other data sets, where relevant), is also shown. All of these values correspond to case ii) described in the text.

obtained by the WMAP collaboration within 1σ, while there is agreement within 2σ and with the constraints obtained with the HST data. The values of Θ also differ at 1σ. Other values of cosmological parameters obtained do agree with the ones obtained by the WMAP collaboration in the context of the standard inflationary scenario. On the other hand, for both models, we found that there is no agreement with the values of A_s obtained in almost all of the cases of fixed values of A explored. This can be understood as due to the fact that the effective amplitude of the

power spectrum of density fluctuations depends on A and A_s, so the parameters act at a certain level as degenerated parameters. However, there is agreement between the values for σ_8[11] obtained and those of the fiducial model. Note, however, that this is a derived parameter which depends on the effective amplitude. It should also be noted that the models included in case i) are preferred by the data as compared to the models included in case ii), as can be inferred from the value of $\chi^2_{\rm min}$ of the respective statistical analyses listed in Tables I, II, and III.

When analyzing the correlations between the cosmological parameters $\Omega_b h^2$, $\Omega_c h^2$ and θ, τ and B, we find that for both Models I and II the values of the correlation coefficient $\rho_{B\theta}$, $\rho_{B\Omega_b h^2}$ and ρ_{BH_0} are positive for positive best-fit values of B, while $\rho_{B\Omega_c h^2}$ is positive for negative best-fit values of B. Furthermore, the correlation is strong for $\Omega_b h^2$, $\Omega_c h^2$ and H_0 while for θ and τ the correlation coefficient is less than 0.3 for all the cases studied in this paper.

VI. SUMMARY AND CONCLUSIONS

In this paper, we have studied the phenomenological predictions of the collapse models developed in Refs. [2,10,27] and incorporated the effect of late-time plasma physics. We have calculated the prediction for the CMB fluctuation spectrum in the case where the collapse of the k modes of the scalar field during the inflationary period is included. Furthermore, we have performed a statistical analysis in order to compare the prediction of the collapse models with recent data from the CMB fluctuation spectrum and the matter power spectrum obtained by the SDSS collaboration, setting bounds on the model parameters A and B that characterize the collapse times of the scalar field modes. Results from the statistical analyses were discussed in Sec. V and can be summarized as follows:

- For $|A| > 20$ in Model I, any value of B provides a good fit to the data within the range studied in this paper ($B = -10^9 \cdots 10^9$).
- For $|A| < 20$ in Model I, there is a nontrivial range of values of B that provide a good fit to the data. However, values of A lying in the range: $10^{-4} < A < 20$ are not viable since the collapse of the modes occurs after the inflationary period. Furthermore, the data indicate that the values in the range $-20 < A < -1$ are preferred.
- The best fit values of B obtained for $|A| < 20$ in Model I lie in the range $B < 1.88$ Mpc.
- In Model II, there is a nontrivial range of values of B that provide a good fit to the data for all values of A tested ($A = -10^9 \cdots 10^9$). However, values of A lying in the range: $10^{-4} < A < 10^9$ are not viable since the collapse of the modes occurs after the inflationary period. Furthermore, the data indicate that the values in the range $|A| > 1$ are preferred.
- The best fit values of B obtained for all values of A studied in this paper for Model II lie in the range $B < 1.88$ Mpc.
- The value obtained for the cosmological parameters is consistent within 3σ with those obtained by the WMAP collaboration assuming a standard inflationary scenario and also with bounds established by BBN and the value of H_0 obtained with the HST.

This analysis allows us to compare the value of the scale factor at the collapse time $a(\eta_k^c)$, with the traditional value of the scale factor at "horizon crossing" which is often set to mark the *quantum to classical transition* in the standard explanation of inflation: a_k^H. The "horizon crossing" occurs when the length corresponding to the mode k has the same size that the Hubble radius H_I^{-1} (in comoving modes, $k = aH_I$) therefore, $a_k^H \equiv a(\eta_k^H) = \frac{k}{H_I} = \frac{3k}{8\pi \rm GV}$. Thus the ratio of the value of the scale factor at horizon crossing for mode k and its value at collapse time is

$$\frac{a_k^H}{a_k^c} = k\eta_k^c(k) = A + Bk. \tag{22}$$

The results discussed in Sec. V show that two cases are consistent with the data: the one for which the collapse time of inflaton field modes is previous to the time of "horizon crossing" of all modes of the inflaton field, and the opposite case. However, the data seem to favor the case in which the collapse happens before the modes cross the horizon.

As we found that there are good fits (for suitable ranges of B) for all values of the parameter A, we must conclude that the existing data do not lead to a preferred scale for the times of collapse of the wave function for the relevant modes. However, for each value of A, interesting bounds can be placed on the value of the parameter B which in this approach characterizes the modifications of the primordial spectral shape with respect to the HZ conventional flat scale-free spectrum.

ACKNOWLEDGMENTS

The authors are grateful to Gabriel León for useful discussions about the collapse models. Numerical calculations were performed with the KANBALAM facility located at UNAM. The authors would like to thank the people of DGSCA-UNAM for computational and technical support. S. J. L. is supported by PICT 2007-02184 from Agencia Nacional de Promoción Científica y Tecnológica, Argentina and by PIP N 11220090100152 from Consejo Nacional de Investigaciones Científicas y Técnicas, Argentina. This work has been partially funded by project AYA2010-21766-C03-02 of the Spanish Ministry of Science and Innovation (MICINN) and by Grant No 101712 from CONACYT (México).

[11] σ_8 is the rms mass fluctuation amplitude in spheres of size $8h^{-1}$ Mpc.

[1] D. Sudarsky, Int. J. Mod. Phys. D **20**, 509 (2011).
[2] A. Perez, H. Sahlmann, and D. Sudarsky, Classical Quantum Gravity **23**, 2317 (2006).
[3] D. Sudarsky, J. Phys. Conf. Ser. **68**, 012029 (2007).
[4] D. Sudarsky, J. Phys. Conf. Ser. **67**, 012054 (2007).
[5] A. Diez-Tejedor, G. León, and D. Sudarsky, arXiv:1106.1176.
[6] R. Penrose, *The Emperor's New Mind. Concerning Computers, Minds and Laws of Physics* (Oxford University Press, New York, 1989).
[7] R. Penrose, in *Physics meets Philosophy at the Planck Scale: Contemporary Theories in Quantum Gravity*, edited by C. Callendar and N. Huggett (2001), pp. 290–+.
[8] L. Diósi, Phys. Lett. A **120**, 377 (1987).
[9] L. Diósi, Phys. Rev. A **40**, 1165 (1989).
[10] A. de Unánue and D. Sudarsky, Phys. Rev. D **78**, 043510 (2008).
[11] A. Diez-Tejedor and D. Sudarsky, arXiv:1108.4928.
[12] G. León, A. De Unánue, and D. Sudarsky, Classical Quantum Gravity **28**, 155010 (2011).
[13] W. H. Kinney, arXiv:0902.1529.
[14] A. Lewis, A. Challinor, and A. Lasenby, Astrophys. J. **538**, 473 (2000).
[15] D. Larson, J. Dunkley, G. Hinshaw, E. Komatsu, M. R. Nolta, C. L. Bennett, B. Gold, M. Halpern, R. S. Hill, N. Jarosik *et al.*, Astrophys. J. Suppl. Ser. **192**, 16 (2011).
[16] B. A. Reid, W. J. Percival, D. J. Eisenstein, L. Verde, D. N. Spergel, R. A. Skibba, N. A. Bahcall, T. Budavari, J. A. Frieman, M. Fukugita *et al.*, Mon. Not. R. Astron. Soc. **404**, 60 (2010).
[17] A. C. S. Readhead *et al.*, Astrophys. J. **609**, 498 (2004).
[18] C. Kuo *et al.* (ACBAR), Astrophys. J. **600**, 32 (2004).
[19] F. Piacentini *et al.*, Astrophys. J. **647**, 833 (2006).
[20] W. C. Jones *et al.*, Astrophys. J. **647**, 823 (2006).
[21] H. C. Chiang, P. A. R. Ade, D. Barkats, J. O. Battle, E. M. Bierman, J. J. Bock, C. D. Dowell, L. Duband, E. F. Hivon, W. L. Holzapfel *et al.*, Astrophys. J. **711**, 1123 (2010).
[22] M. L. Brown, P. Ade, J. Bock, M. Bowden, G. Cahill, P. G. Castro, S. Church, T. Culverhouse, R. B. Friedman, K. Ganga *et al.*, Astrophys. J. **705**, 978 (2009).
[23] A. Lewis and S. Bridle, Phys. Rev. D **66**, 103511 (2002).
[24] G. Miele and O. Pisanti, Nucl. Phys. B, Proc. Suppl. **188**, 15 (2009).
[25] G. Steigman, arXiv:1008.4765.
[26] A. G. Riess *et al.*, Astrophys. J. **699**, 539 (2009).
[27] A. de Unánue and D. Sudarsky, Phys. Rev. D **78**, 043510 (2008).